GEOPHYSICS, VOL. 81, NO. 6 (NOVEMBER-DECEMBER 2016); P. J79–J86, 3 FIGS., 1 TABLE.
10.1190/GEO2015-0697.1

Attributes of the magnetic field, analytic signal, and monogenic signal for gravity and magnetic interpretation

Xiong Li[1] and Mark Pilkington[2]

ABSTRACT

Many of the transforms and attributes used in gravity and magnetic interpretation can be expressed as a 2D or 3D vector. The horizontal gradient and the 2D analytic signal are 2D vectors. The gravity or magnetic field, the 3D analytic signal, and the monogenic signal are defined by a 3D vector. In practice, we prefer to interpret the amplitude and/or phase of a 2D or 3D vector, but we often forget that a meaningful interpretation requires a magnetic reduction-to-the-pole operation when these techniques are applied to magnetic anomaly data and the source body is 3D. Furthermore, the gravity or magnetic anomaly has an unknown constant level that may affect the amplitude and phase. The horizontal gradient, the analytic signal, and the monogenic signal can be applied to not only the gravity or magnetic anomaly but also any nth-order derivative or a filtered version of the anomaly. They can be related to each other and to the magnetic field vector. We do not introduce new attributes. Instead, we have explained the relationships among different transforms (or vectors) and addressed precautions and requirements for their practical use.

INTRODUCTION

A 2D vector has two orthogonal components, whereas a 3D vector has three. The three derivatives of the gravity or magnetic potential constitute the three components of the 3D gravity or magnetic field vector. We may further compute the three derivatives of a component of a field vector or a gradient tensor, and it still results in a 3D vector. A 2D or 3D vector can also be fully defined by its amplitude and phase. For structural interpretation, we may prefer the amplitude and/or phase to a single derivative. Different terms are often applied to the amplitude and phase depending on their associated mathematical transform and signal. The magnitude and phase of the 2D horizontal gradient vector were historically used together during torsion balance times, but only the magnitude has been interpreted during the spring-based relative gravimeter era. The amplitude and phase of the 2D and 3D analytic signal have been studied extensively and have found applications in a wide variety of areas. The Hilbert transform may have become the most important mathematical tool to define the analytic signal (Nabighian, 1972, 1974, 1984). Researchers continue constructing new signals using different transforms, e.g., the Riesz transform for the monogenic signal (Felsberg and Sommer, 2001). Hassan and Yalamanchili (2013) recently apply the monogenic signal to interpretation of magnetic anomaly data. Hidalgo-Gato and Barbosa (2015) focus on the local phase of the monogenic signal of a band-pass filtered version of the total magnetic intensity (TMI) anomaly.

There is an increasing number of seismic attributes. Barnes (2007) argues that duplicate attributes are legion, and many seismic attributes are redundant. The same argument can be applied to gravity and magnetic transforms, filters, and attributes (Pilkington and Keating, 2009). For example, the attributes of the monogenic signal are not really new to gravity and magnetic interpretation; they are just the components of the horizontal gradient vector (a 2D vector) and the 3D complex analytic signal (a 3D vector). This work reviews and links routinely used and new concepts regarding several attributes, compares them with the components of the magnetic field vector, and discusses their practical uses.

THE 3D MAGNETIC FIELD VECTOR

The magnetic (or gravity) field is conservative and described by a 3D vector that is formed from the three derivatives of the scalar magnetic (or gravity) potential. These derivatives are called the north, east, and vertical components. The magnetic field can be fully defined either by these three orthogonal components or by three other parameters: the total field (F, i.e., TMI), magnetic in-

Manuscript received by the Editor 18 December 2015; revised manuscript received 6 July 2016; published online 10 October 2016.
[1]CGG, Houston, Texas, USA. E-mail: xiong.li@cgg.com.
[2]Geological Survey of Canada, Ottawa, Ontario, Canada. E-mail: mark.pilkington@canada.ca.

clination I, and magnetic declination D (Figure 1a and Table 1). The horizontal component H and the declination D are the magnitude and phase of the 2D vector formed by the horizontal north and east components. The total field F and the inclination I are equal to the amplitude and phase of the 3D magnetic field vector, respectively. Different terms in some routinely used gravity and magnetic interpretation techniques are linked to these amplitude (or magnitude) and phase attributes (Figure 1 and Table 1).

THE 2D HORIZONTAL GRADIENT VECTOR

The horizontal gradient vector of the gravity anomaly was used in the first half of the last century to interpret gravity gradient data measured by the torsion balance. We routinely call the magnitude of the horizontal gradient vector the horizontal gradient, i.e., omitting the term "magnitude." The phase of the horizontal gradient vector is also called the azimuth. When the 2D horizontal gradient vector is applied to the magnetic potential, the horizontal gradient magnitude (HGM) is just the horizontal component H of the magnetic field, and the azimuth is called the magnetic declination D (Figure 1a and Table 1).

In historical interpretation of torsion balance data, the horizontal gravity vectors are plotted as arrows. The length of an arrow is proportional to the magnitude of the horizontal gradient vector, and the direction of an arrow is the azimuth of the vector (Heiland, 1946). In such a plot, all arrows point to a positive anomalous mass (Figure 2) and away from a negative anomalous mass. This helps in locating source bodies in particular.

The HGM can be applied directly to the gravity or vertical gravity gradient anomaly for edge detection. However, we must compute the magnetic potential or magnetic reduction-to-the-pole (RTP) anomaly first, when the HGM is applied to the TMI anomaly (Cordell and Grauch, 1985; Grauch et al., 2001). An exception may be where the magnetic inclination is very high (e.g., $> 60°$) and remanent magnetization is insignificant or parallel with the present geomagnetic field direction. The magnetic potential is the vertical integral of the magnetic RTP anomaly. The magnetic RTP result is equivalent to the vertical gravity gradient, and the magnetic potential to the pseudogravity, except for a scaling factor difference. Some workers may prefer to use the magnetic potential over the pseudogravity for interpretation or further transformation, which avoids difficulty with determination of a proper scaling factor.

The HGM is also widely used for edge detection in image processing. In seismic interpretation, Dalley et al. (1989) compute the two horizontal derivatives of a time horizon and define the dip and azimuth attributes. They correspond to the magnitude and azimuth of the horizontal gradient vector.

THE HILBERT TRANSFORM AND THE COMPLEX ANALYTIC SIGNAL

Nabighian (1972, 1974) pioneers the application of the analytic signal to magnetic interpretation. The Hilbert transform plays an important role in the definition and application of the analytic signal. The complex analytic signal $\mathbf{AS}[f(x)]$ of a real function $f(x)$ is defined as

$$\mathbf{AS}[f(x)] = f(x) - i\mathbf{H}[f(x)], \tag{1}$$

where $i = \sqrt{-1}$ and $\mathbf{H}[f(x)]$ is the Hilbert transform of $f(x)$. If $\mathbf{F}[f(x)]$ is the Fourier transform of $f(x)$, $\mathbf{H}[f(x)]$ and $\mathbf{F}[f(x)]$ are related by

$$\mathbf{H}[f(x)] = i\,\mathrm{sgn}(k)\mathbf{F}[f(x)], \tag{2}$$

where k is the wavenumber. Thus, the 2D Hilbert transform operator in the wavenumber domain is

$$H_T = i\,\mathrm{sgn}(k). \tag{3}$$

For a profile data set measured on a horizontal surface, the two derivatives of an observed magnetic anomaly form a 2D vector and a Hilbert transform pair

Table 1. The amplitude and phase of 2D and 3D vectors applied to the magnetic field, the horizontal gradient vector and the 3D complex analytic signal, and the monogenic signal (Figure 1). The names may be different, but they have the same geometric meaning. The tilt angle and the instantaneous (local) phase are complementary by definition. The two first-order Riesz transforms r_x and r_y are equivalent to the x- and y-components of the 3D Hilbert transform introduced by Nabighian (1984).

	Magnetic field	Horizontal gradient vector and complex analytic signal	Monogenic signal
Input	Potential U	Potential field anomaly f	Function $f(x, y)$
Three components	Three derivatives of U (X, Y, Z)	Three derivatives of f ($\frac{\partial f}{\partial x}$, $\frac{\partial f}{\partial y}$, $\frac{\partial f}{\partial z}$)	f and its two first-order Riesz transforms (f, r_x, r_y)
Magnitude of 2D vector	Horizontal component $H = \sqrt{X^2 + Y^2}$	HGM $= \sqrt{\left(\frac{\partial f}{\partial x}\right)^2 + \left(\frac{\partial f}{\partial y}\right)^2}$	The Riesz transform magnitude $q = \sqrt{r_x^2 + r_y^2}$
Phase of 2D vector	Magnetic declination $D = \tan^{-1}(Y/X)$	Horizontal gradient azimuth $\phi = \tan^{-1}\left(\frac{\partial f}{\partial y} / \frac{\partial f}{\partial x}\right)$	Instantaneous (local) orientation $\theta = \tan^{-1}(r_y/r_x)$
Amplitude of 3D vector	Total field $F = \sqrt{X^2 + Y^2 + Z^2}$	ASA $= \sqrt{\left(\frac{\partial f}{\partial x}\right)^2 + \left(\frac{\partial f}{\partial y}\right)^2 + \left(\frac{\partial f}{\partial z}\right)^2}$	Instantaneous (local) amplitude $A = \sqrt{r_x^2 + r_y^2 + f^2}$
Phase of 3D vector	Magnetic inclination $I = \tan^{-1}(Z/\sqrt{X^2 + Y^2})$	Tilt angle $\theta = \tan^{-1}\left(\frac{\partial f}{\partial z} / \sqrt{\left(\frac{\partial f}{\partial x}\right)^2 + \left(\frac{\partial f}{\partial y}\right)^2}\right)$	Instantaneous (local) phase $\phi = \tan^{-1}\left(\sqrt{r_x^2 + r_y^2}/f\right)$

$$\mathbf{F}\left[\frac{\partial f}{\partial z}\right] = -i\,\mathrm{sgn}(k)\mathbf{F}\left[\frac{\partial f}{\partial x}\right]. \quad (4)$$

This leads to a 2D complex analytic signal in which the real part is the horizontal derivative of the TMI anomaly and the imaginary part is the vertical derivative (Nabighian, 1972)

$$\mathbf{AS}\left[\frac{\partial f}{\partial x}\right] = \frac{\partial f}{\partial x} + i\frac{\partial f}{\partial z}. \quad (5)$$

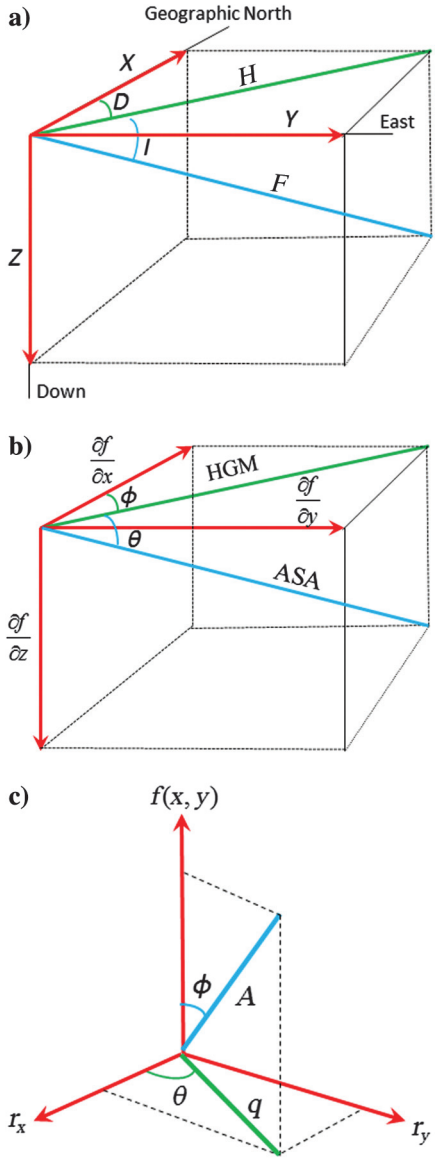

Figure 1. Concepts and relationships of (a) the magnetic field, (b) the 2D horizontal gradient vector and the 3D analytic signal of a potential field anomaly f, and (c) the monogenic signal of function $f(x, y)$. The terms r_x and r_y of the monogenic signal are the two first-order Riesz transforms, i.e., the x- and y-derivatives of the vertical integral of the input function $f(x, y)$. See Table 1 for the definition of the input function and the components of the 2D and 3D vectors in each of the three cases and their comparison.

Comparing equation 5 with equation 1, we can see that the 2D analytic signal we routinely call is really the analytic signal of the horizontal derivative of the magnetic anomaly, not the analytic signal of the anomaly itself. In fact, the Hilbert transform pair holds for, the analytic signal can be composed of, and function f in Figure 1b can be, any potential function: the potential, a component of a field vector, a component of a gradient tensor, nth-order derivative of a gradient component, or a low- or high- or band-pass-filtered result of any one of these. The Hilbert transform is a useful mathematical tool to link and convert derivatives of the same function. For geophysical interpretation, it is the amplitude and phase of the 2D or 3D analytic signal vector being used.

Nabighian (1972, 1974) considers the amplitude of the complex analytic signal of the TMI anomaly due to a 2D body, and he proves that the analytic signal amplitude (ASA) is independent of the direction of the ambient magnetic field and the direction of source magnetization. He shows that the horizontal position and depth of vertices of a 2D polygonal body with uniform magnetization can be estimated through simple examination of the ASA along the profile. Thurston and Smith (1997) use the local wavenumber of the TMI anomaly due to a 2D body and show that the local wavenumber has the same independence. The local wavenumber is the horizontal derivative of the local phase of the complex analytic signal.

Nabighian (1984) extends the complex analytic signal from 2D (for a profile data set) to 3D (for a gridded data set) by the introduction of a generalized signum function:

$$\mathrm{sgn}(u, v) = \frac{u}{\sqrt{u^2 + v^2}}\mathbf{e}_x + \frac{v}{\sqrt{u^2 + v^2}}\mathbf{e}_y, \quad (6)$$

where $\mathbf{e}_x$ and $\mathbf{e}_y$ are the unit vectors and u and v are the wavenumbers in the x- and y-directions, respectively. The generalization of the 2D Hilbert transform operator is written for 3D as

$$H_T = -i\,\mathrm{sgn}(u, v) = H_1\mathbf{e}_x + H_2\mathbf{e}_y, \quad (7)$$

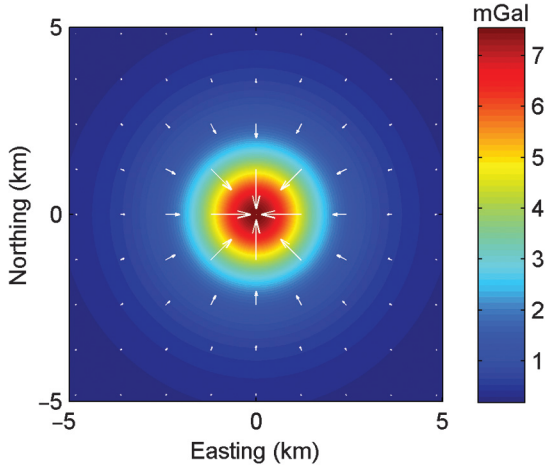

Figure 2. The gravity anomaly of a vertical cylinder and its horizontal gradient vector. The cylinder model is the same as in Figure 3, and the density contrast is 1 g/cm^3. The length of the arrow is proportional to the HGM of the gravity anomaly that is shown in Figure 3g.

$$H_1 = -\frac{iu}{\sqrt{u^2+v^2}}, \tag{8a}$$

$$H_2 = -\frac{iv}{\sqrt{u^2+v^2}}, \tag{8b}$$

where H_1 and H_2 are the x- and y-components of the 3D Hilbert transform operator. It is evident that H_1 and H_2 are the wavenumber operators that calculate the x- and y-derivatives from the vertical derivative of a potential function $f(x,y)$, except for a sign reversal. Thus, the x- and y-components of the 3D Hilbert transform of $f(x,y)$ are

$$H_x(f) = \mathbf{F}^{-1}[H_1\mathbf{F}(f)], \tag{9a}$$

$$H_y(f) = \mathbf{F}^{-1}[H_2\mathbf{F}(f)], \tag{9b}$$

where $\mathbf{F}^{-1}$ stands for the inverse Fourier transform.

The three derivatives in the wavenumber domain are linked via the Hilbert transform

$$\mathbf{F}\left(\frac{\partial f}{\partial z}\right) = H_1\mathbf{F}\left(\frac{\partial f}{\partial x}\right) + H_2\mathbf{F}\left(\frac{\partial f}{\partial y}\right). \tag{10}$$

Equation 10 is used in practice to compute the vertical derivative from the two horizontal derivatives. This computation is very stable because H_1 and H_2 are phase transforms.

Roest et al. (1992) are among the first to use the term of the 3D analytic signal. They clearly define the three orthogonal components of the 3D analytic signal to be the three orthogonal derivatives

$$\mathbf{AS} = \frac{\partial f}{\partial x}\mathbf{e}_x + \frac{\partial f}{\partial y}\mathbf{e}_y + i\frac{\partial f}{\partial z}\mathbf{e}_z, \tag{11}$$

and the ASA in 3D as the total gradient (see Table 1). In fact, the 3D ASA is preferably called the total gradient in gravity and magnetic interpretation. Miller and Singh (1994) introduce the tilt angle that is the local phase of the 3D analytic signal. Figure 1b and Table 1 define the elements (or attributes) of the complex analytic signal in the 3D case. For the 3D analytic signal of the magnetic potential, its ASA is the total field F and its tilt angle is the magnetic inclination I.

Many different variants of the tilt angle have been used in gravity and magnetic interpretation because the tilt angle has an automatic gain control effect and resolves shallow and deep bodies equally well. The tilt angle varies from $-90°$ to $+90°$. Wijns et al. (2005) define the theta angle as the arccosine of the ratio of the HGM to the ASA, so the theta angle is thus the absolute value of the tilt angle. In fact, Wijns et al. (2005) use for edge detection the so-called theta map, which is the cosine of the theta angle

$$\cos(\theta) = \sqrt{\left(\frac{\partial f}{\partial x}\right)^2 + \left(\frac{\partial f}{\partial y}\right)^2} \Big/ \sqrt{\left(\frac{\partial f}{\partial x}\right)^2 + \left(\frac{\partial f}{\partial y}\right)^2 + \left(\frac{\partial f}{\partial z}\right)^2}. \tag{12}$$

The theta map values vary from zero to one. The tilt angle is the vertical derivative normalized by the HGM, i.e., the angle measured from the horizontal plane (Table 1). The angle TDX in Cooper and Cowan (2006) is the HGM normalized by the absolute value of the vertical derivative

$$\mathrm{TDX} = \tan^{-1}\left(\sqrt{\left(\frac{\partial f}{\partial x}\right)^2 + \left(\frac{\partial f}{\partial y}\right)^2} \Big/ \left|\frac{\partial f}{\partial z}\right|\right). \tag{13}$$

Thus, the angle TDX deviates from the vertical and has values between 0° and 90°. Li (2006b) discusses the relationship among different angles.

Interpreters use the minima (0°) of the absolute value of the tilt angle or the maxima (90°) of the TDX or the maxima (1.0) of the theta map for edge detection. This is equivalent to using the zero contours of the vertical derivative. We have been using the zeros of the vertical derivative of the gravity anomaly for determining the location of the fault for many decades (Evjen, 1936). We do not use the zeros of the TMI anomaly or even the zeros of the vertical derivative of the TMI anomaly without a magnetic RTP. Unfortunately, the relationship between the zeros of the tilt angle and the vertical derivative and the magnetic RTP requirement is often forgotten (Miller and Singh, 1994; Wijns et al., 2005; Cooper and Cowan, 2006).

When Nabighian (1972, 1974) develops the analytic signal for magnetic interpretation, the analytic signal was also applied to seismic data almost at the same time. According to Ulrych et al. (2007), this application was first reported internally at Seiscom in 1972, and Norman Neidel later suggested using the Hilbert transform. An easy-to-access reference appeared seven years later (Taner et al., 1979). In this analysis, the seismic trace amplitude is treated as the real part of the complex analytic signal, whereas the imaginary part of the signal is computed by taking its Hilbert transform. The amplitude, local phase, and local wavenumber known in gravity and magnetic applications are called the instantaneous envelope, phase, and frequency in the seismic attribute analysis, respectively.

Equation 5 for the 2D case and equation 11 for the 3D case indicate that the analytic signal we routinely refer to is strictly speaking the analytic signal of a gradient of the magnetic anomaly, not the analytic signal of the anomaly itself. In gravity and magnetics, we may also compute the analytic signal of the nth-order derivative of the anomaly (Hsu et al., 1996). MacLeod et al. (1993) compute the vertical integral of the TMI anomaly, then calculate the ASA of the vertical integral, and show how this ASA can reduce the effect of the magnetization direction. Cooper (2014) calls (the amplitude of) the analytic signal of the vertical integral of the TMI anomaly the zero-order analytic signal. In fact, this is truly the analytic signal of the TMI anomaly according to the definition in equation 1. Thus, Luo et al. (2011) call it the direct analytic signal of the potential field anomaly f and define the 3D direct analytic signal as follows:

$$\mathbf{DAS} = H_x(f)\mathbf{e}_x + H_y(f)\mathbf{e}_y + if\mathbf{e}_z. \tag{14}$$

Luo et al. (2011) apply the 3D direct analytic signal to magnetic RTP results and compute the amplitude, HGM, tilt angle, and theta map of the 3D direct analytic signal.

THE RIESZ TRANSFORM AND THE MONOGENIC SIGNAL

The recent application of the monogenic signal to interpretation of magnetic data by Hassan and Yalamanchili (2013) and Hidalgo-

Gato and Barbosa (2015) follows the definition of the monogenic signal in Felsberg and Sommer (2001). In their conclusions, Felsberg and Sommer (2001, p. 3143) write, "In the present paper, we have analytically derived the monogenic signal, which is a generalization of the analytic signal to two dimensions. This new 2D analytic signal is based on the Riesz transform and preserves the properties of the 1D analytic signal." There is a difference in the dimensionality when computer scientists and geophysicists label the Hilbert or Riesz transform and the analytic or monogenic signal. The 1D in Felsberg and Sommer (2001) is the 2D in Nabighian (1972) and is for a profile data set, and the 2D in Felsberg and Sommer (2001) is the 3D in Nabighian (1984) and is for a gridded data set.

In the mathematical theory of harmonic analysis, the Hilbert transform is applicable to Euclidean spaces of dimension $d = 1$ only, and the Riesz transforms are a family of generalizations of the Hilbert transform to dimension $d > 1$ (Riesz, 1928). Stein and Weiss (1971, p. 224) define clearly the first-order Riesz transforms of dimension d as a function of the wavenumbers k_j in the Fourier transform, and these first-order Riesz transform operators R_j are

$$R_j = -ik_j/\sqrt{\sum_{l=1}^{d} k_l^2}, \quad j = 1, 2, \ldots, d. \tag{15}$$

Evidently, the first-order 2D Riesz transform operators are identical to, including the sign, the x- and y-components of the 3D Hilbert transform operator of Nabighian (1984), which is given in equation 8. Felsberg and Sommer (2001, p. 3139) reverse the sign. Hidalgo-Gato and Barbosa (2015) follow Felsberg and Sommer (2001), and their equation 13 defines the x- and y-components of the first-order Riesz transform operator and is the same as equation 8 in this work except for a sign reversal. This sign difference is insignificant because we use and interpret the local amplitude and local phase, not the x- and y-components themselves.

Nabighian (1984) is not aware of the existence of the Riesz transforms when he generalizes the 2D Hilbert transform to the 3D Hilbert transform (M. N. Nabighian, personal communication, 2015). Felsberg and Sommer (2001) review different approaches (partial Hilbert transform, total Hilbert transform, and a combination of them) in generalizing the Hilbert transform to higher dimensions and state their limitations regarding completeness and isotropy properties. They reference Nabighian (1984) and obtain relations (their equations 8 and 9) that are the same as the 3D Hilbert transform (equation 9), but they still define the monogenic signal using the Riesz transforms r_x and r_y, not using its equivalent, the 3D Hilbert transform H_x and H_y. Clearly speaking, the monogenic signal can be defined by

$$\mathbf{MS} = f\mathbf{e}_z + i\lfloor H_x(f)\mathbf{e}_x + H_y(f)\mathbf{e}_y \rfloor. \tag{16}$$

Evidently, the (complex) monogenic signal (equation 16) is the same as the (complex) zero-order or direct analytic signal (equation 14) except for a switch of the real and imaginary parts. This switch is not important because we use the magnitude, amplitude, and phase of the three orthogonal components of the monogenic signal or the 3D direct analytic signal of a gravity or magnetic anomaly grid. The monogenic signal treats an input image (grid) as the real part of the complex analytic signal, and the imaginary part consists of the two first-order Riesz (i.e., 3D Hilbert) transforms. This is consistent with the analytic signal used in seismic analysis.

Felsberg and Sommer (2001) do not realize the existence of the 3D analytic signal defined by Roest et al. (1992) and our popular use in gravity and magnetic interpretation of the amplitude and phase attributes of the 3D analytic signal. Comparing Figure 1b and 1c and reading Table 1, the Riesz transform magnitude q and the instantaneous (or local) orientation θ of the monogenic signal of the input grid $f(x, y)$ (Hassan and Yalamanchili, 2013) are the magnitude (HGM) and phase (azimuth ϕ) of the 2D horizontal gradient vector of the vertical integral of the same input grid $f(x, y)$. The instantaneous (local) amplitude A of the monogenic signal of the input grid $f(x, y)$ (Hassan and Yalamanchili, 2013) is the ASA of the vertical integral of the same input grid $f(x, y)$. The directional Hilbert attribute H_θ in Hassan and Yalamanchili (2013) is a combination of the two horizontal gradient components and the phase of the horizontal gradient vector, and it is similar to the rotation of different gradient components that are used to interpret gravity gradient data (Dickinson et al., 2009).

The instantaneous (local) phase ϕ of the monogenic signal, like the angle TDX in Cooper and Cowan (2006), is the angle measured from the vertical; but unlike TDX, it is normalized by the input function itself and not by its absolute value. The tilt angle θ of the 3D analytic signal and the local phase ϕ of the monogenic signal range from $-90°$ to $+90°$, and they are complementary by definition. The tilt angle varies continuously but the local phase changes abruptly from $-90°$ to $+90°$ across the zero contour of the input grid $f(x, y)$.

APPLICATIONS TO MAGNETIC ANOMALIES

As explained previously, a direct application of the monogenic signal to the TMI anomaly is equivalent to computation of the 2D horizontal gradient vector and the routinely used 3D complex analytic signal of the vertical integral of the TMI anomaly. When the monogenic signal is applied to the magnetic RTP anomaly, the five attributes that Hassan and Yalamanchili (2013) use (Figure 1c) are equivalent to the components (Figure 1b) of the horizontal gradient vector and the routinely called complex analytic signal of the magnetic potential anomaly. When the monogenic signal is applied to the gravity anomaly, it is equivalent to computing the components of the horizontal gradient vector and the routinely called analytic signal of the gravity potential. One may derive the vertical component of the anomalous magnetic field from the observed TMI anomaly. If one computes the monogenic signal of the vertical magnetic component, the attributes of the monogenic signal (Figure 1c) are equivalent to the components of the magnetic field (Figure 1a).

For applications in image processing, brightness or intensity is often used to quantify a general gray-scale image (including seismic profiles) that is defined by gray levels. Importantly, the gray levels are positive integers only. Therefore, caution must be exercised, when a transformation commonly used in image processing is applied to gravity and magnetic data. Unlike a general gray-scale image, a gravity or magnetic anomaly grid can have positive and negative values. Furthermore, these values have a relative, not absolute, meaning and include an unknown direct current (DC) level.

The anomaly is relative not absolute

When the monogenic signal is applied to magnetic anomalies, its local phase has a value between 0° and +90°, if the input anomaly value is positive and a value between 0° and −90°, if the input anomaly value is negative (see Table 1). The local phase jumps from −90° to +90° abruptly, when the anomalies change the sign from negative to positive, i.e., across the horizontal plane (Figure 3c and 3f). Hassan and Yalamanchili (2013) display particularly enlarged images of the local phase. The 180° change or the 90° absolute maximum in the local phase occurs at the zero contour of the magnetic anomaly. However, there is no theoretical basis to justify the use of such a change for the detection of edges and delineation of geologic structures. The zero value may be a true zero in gravity and magnetic model simulations, but the observed gravity and magnetic anomalies are relative to some chosen reference level. An anomaly grid may have positive and negative values, or it may be completely positive or completely negative, depending on processing steps and conventions used.

The DC level in the gravity or magnetic anomaly grid $f(x, y)$ will also affect the values of the other four attributes of the monogenic signal (see Table 1). The horizontal gradient vector and the complex analytic signal of the gravity or magnetic anomaly require the three orthogonal first-order derivatives of the anomaly, and they are thus not affected by the DC value in the anomaly grid. Consequently, it is better to use the horizontal gradient vector and the routine analytic signal of the observed anomaly than the monogenic signal of the observed anomaly for interpretation. Luo et al. (2011) demonstrate that the 3D direct analytic signal (i.e., the monogenic signal) is less sensitive to noise in data than the routinely used analytic signal, but they fail to explain the effects of the DC level. If noise amplification in the computation of derivatives is a concern, one may apply a low-pass filter to the observed anomaly first. Cooper and Whitehead (2016) notice that the zero-order analytic signal requires the correct removal of the regional magnetic field from the data. The regional field may contain, but is often more than, a DC shift. To our knowledge, the regional field affects many techniques or algorithms for qualitative and quantitative interpretation, but the DC level affects none of the routinely or widely used techniques or algorithms.

Magnetic RTP is required

Like the HGM, the analytic signal and the monogenic signal may be applied directly to gravity or vertical gravity gradient data for which an anomaly is positioned directly over its causative source. It is often dangerous to apply them to the TMI anomaly directly, without a magnetic RTP or magnetic potential (pseudogravity) computation first. Most transformations used for edge detection are to some degree affected by nonvertical magnetization for 3D cases and nonvertical dips for 2D and 3D cases (Pilkington and Keating, 2009). Hence, RTP of the magnetic data should be done to mitigate these effects. Even so, the RTP result still suffers from an unknown DC level.

Neither Hassan and Yalamanchili (2013) nor Hidalgo-Gato and Barbosa (2015) state explicitly the prerequisite for magnetic RTP. Their synthetic models assume either a vertical magnetization for 3D bodies or a 2D geometry. Hidalgo-Gato and Barbosa (2015) compute the local phase of the monogenic signal of the TMI anomaly over the Pará-Maranhão Basin, Brazil. The magnetic inclination in the area is −1.9°, i.e., near the magnetic equator. It represents a challenging area. On the one hand, an accurate magnetic RTP computation at such a low latitude is extremely difficult. On the other hand, the magnetic anomaly does not indicate dominant 2D structures, so the field-data application of Hidalgo-Gato and Barbosa (2015) could lead to mislocated edges because of inclination effects. The magnetic anomaly near the magnetic equator (or the magnetic reduction-to-the-equator result) has some artifacts and can mislead interpretation (e.g., see Figure 14 of Li, 2008).

We use a vertical cylinder model to demonstrate the effect of the direction of magnetization (Figure 3). A vertical cylinder is chosen because it has edges at all orientations. The radius, height, and depth to the top of the cylinder are all 1 km. The observation grid is centered on the axis of the vertical cylinder and has 1001 rows by

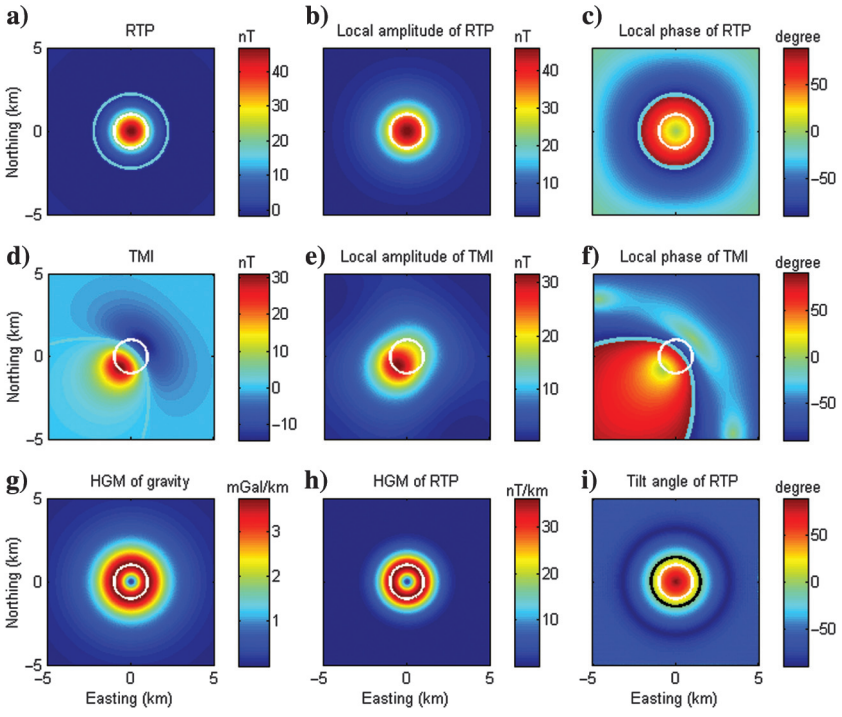

Figure 3. A vertical cylinder model test. The radius, height, and depth to the top of the cylinder are all 1 km. The observation grid has 1001 rows × 1001 columns and a grid spacing of 0.01 km. The outlines of the cylinder are shown as the centered white cycle. (a) The magnetic responses for a vertical magnetization direction, (b) the local amplitude, and (c) the local phase of the monogenic signal of the magnetic RTP-equivalent result in (a). (d) The TMI responses for a magnetic inclination of 45° and a magnetic declination of 45°, (e) the local amplitude, and (f) the local phase of the monogenic signal of the TMI responses in (d). (g) The HGM of the gravity in Figure 2. (h) The HGM and (i) the tilt angle of the magnetic RTP result in (a). The contour line in cyan in (a and d) represents zero and in (c and f) marks the abrupt change from −90° to +90°. The black contour in (i) represents zero.

1001 columns and a grid spacing of 0.01 km. We assume a purely induced magnetization, the magnitude of the geomagnetic field is 40,000 nT, and the magnetic susceptibility of the cylinder is 1000 micro-cgs units (12.57×10^{-3} SI units). Figure 3a shows the magnetic responses for a vertical magnetization direction. Figure 3b and 3c depicts the local amplitude and the local phase, respectively, of the monogenic signal of this magnetic RTP-equivalent result. They are equivalent to the ASA and the complementary angle of the tilt angle of the magnetic potential or pseudogravity anomaly. The 180° change in the local phase (i.e., the zero contour of the tilt angle of the magnetic potential or pseudogravity) is offset away from the true edge of the cylinder because the height of the cylinder is the same as (not much greater than) its top depth.

We then use a magnetic inclination of 45° and a magnetic declination of 45°. Figure 3d, 3e, and 3f displays the TMI responses; the local amplitude and the local phase of the monogenic signal of the TMI responses, respectively. It is clearly seen that the local phase reaches its absolute maximum (90°) and changes 180° (Figure 3c and 3f), where the magnetic anomaly is zero (Figure 3a and 3d). In addition, Figure 3d and 3f shows that the monogenic signal depends on the magnetization direction.

Figure 3g depicts the HGM of the gravity anomaly in Figure 2 (equivalent to the pseudogravity or magnetic potential). Figure 3h shows the HGM of the magnetic RTP result in Figure 3a (equivalent to the vertical gravity gradient). The HGM maxima of the gravity (or pseudogravity) are routinely used for edge detection. This model test indicates that the HGM of the vertical gravity gradient detects edges better than the HGM of the gravity. Basically, the vertical gravity gradient has a better resolution than the gravity when the vertical extension of the body is not much greater than the depth to the top of the body and when several edges are close together (Grauch et al., 2001; Li, 2016).

Figure 3i displays the tilt angle of the magnetic RTP result in Figure 3a. For this vertical cylinder model, the zero-tilt angle of the analytic signal (Figure 3i) matches the true edge more closely than the 180° abrupt change in the local phase of the monogenic signal (Figure 3c) does. This can be explained by the same vertical derivative/integral relationship above. Figure 3c shows the complementary angle of the tilt angle of the vertical integral of the magnetic RTP result in Figure 3a.

Li (2006a) demonstrates that the ASA is not independent of the direction of the ambient magnetic field and the direction of magnetization for the general 3D case. In terms of centering the anomaly over its causative source, however, the 3D ASA can be advantageous over the TMI anomaly itself. Comparing Figure 3a, 3d, and 3e, this conclusion is also true for the local amplitude of the monogenic signal of the TMI anomaly. This suggests that in the absence of remanent magnetization information and/or at low latitudes, the 3D ASA and the local amplitude of the monogenic signal present a possibility of enhanced interpretation, although they lack the resolution that derivative results provide and the structural and textural information that the TMI and RTP anomalies contain. However, the local phase of the monogenic signal of the TMI anomaly has a much stronger dependence on the direction of the ambient magnetic field and the direction of magnetization for the 3D case (Figure 3f). The same is true for the tilt angle of the 3D analytic signal. It is inappropriate and inaccurate to use a characteristic contour (the abrupt 180° change) in the local phase for structural interpretation.

Upward continuation as a low-pass filter

Hidalgo-Gato and Barbosa (2015) compute the local phase of the monogenic signal of a band-pass filtered result of the TMI anomaly and show that this local phase performs better than the tilt angle of the TMI anomaly itself. This band-pass filter is given in Felsberg and Sommer (2004), and it is called the Poisson's scale-space representation. In fact, it is just equivalent to the difference between the TMI anomaly upward continued to two separate levels. Differencing upward continued fields is the separation filter that was introduced for gravity and magnetic interpretation almost 30 years ago (Jacobsen, 1987). The better performance in terms of suppressing random noise and short-wavelength signals can be understood as follows. Their preferred local phase is the same as the complementary angle of the tilt angle of the vertical integral of the difference between upward continued fields at two levels of the TMI anomaly. Differencing means that the use of the monogenic signal by Hidalgo-Gato and Barbosa (2015) does not suffer from an unknown DC level. If the vertical separation between two continuation levels is small, the difference at two levels is equivalent to an upward-continued vertical derivative except for a constant scaling difference. The scaling factor is the vertical separation. This constant scaling factor does not affect use of the monogenic signal for qualitative interpretation. In the field data example of Hidalgo-Gato and Barbosa (2015), they use continuation distances of 0.4 and 0.5 km (the vertical separation thus being 0.1 km), whereas the anomaly grid has a spacing of 0.5 km. The effects of a vertical integral and a vertical derivative are cancelled. In other words, their preferred local phase is just the complementary angle of the tilt angle of an upward continued TMI anomaly. The upward continuation produces a result that is smoother and less sensitive to random noise than the original anomaly, but will not change the primary shapes. The continuation distance is a critical parameter, but Hidalgo-Gato and Barbosa (2015) do not give a clear criterion for its choice.

CONCLUSIONS

The first-order Riesz transforms used to define the monogenic signal for general image processing are the same as the 3D Hilbert transform generalized from the 2D Hilbert transform for gravity and magnetic interpretation. The routinely called 3D analytic signal can be defined by a 3D vector that consists of the three orthogonal derivatives of the potential field anomaly, and it is exactly the 3D analytic signal of the vertical derivative of the anomaly. The three components of the monogenic signal include the anomaly itself and the two horizontal derivatives of the vertical integral of the same anomaly, and the monogenic signal is the same as the 3D direct or zero-order analytic signal of the anomaly. The attributes of the monogenic signal of the magnetic anomaly are equivalent to the attributes of the 2D horizontal gradient vector and the 3D analytic signal of the vertical integral of the magnetic anomaly. The monogenic signal of the vertical component of the magnetic anomaly is equivalent to the components of the magnetic field.

The 180° change or the absolute maximum (90°) in the local phase of the monogenic signal occurs at the zero contour of an anomaly grid. There is no theoretical basis to use this change for edge detection. The observed gravity or magnetic anomaly is a relative anomaly and always suffers from a DC level shift. This DC level affects all attributes of the monogenic signal. The 2D horizontal gradient vector and the routinely used 3D complex analytic

signal of the gravity or magnetic anomaly are not affected by this DC level because they use the three derivatives of the anomaly grid, and perform better than the monogenic signal for gravity and magnetic interpretation. The DC level can also be removed by a band-pass filtering.

The HGM, local phase, and ASA are three popularly used attributes. It is a well-accepted practice to compute the HGM (equivalently, the Riesz transform magnitude) of a magnetic RTP result not the TMI anomaly itself. The local phase of the 3D vector is used in many different variants: the tilt angle, theta map, TDX, instantaneous phase, etc. All of them are strongly affected by the direction of the ambient magnetic field and the direction of magnetization, when the source body is 3D. Therefore, their direct application to the TMI anomaly without a magnetic RTP operation often leads to mislocated source edges. Relatively speaking, the 3D ASA has the weakest dependence on the direction of the ambient magnetic field and the direction of magnetization. The 3D ASA is good for centering an anomaly over its causative source but poor for delineating structural details.

There are a great number of existing filters and attributes in gravity and magnetic interpretation. This number or list keeps growing. To make the list more manageable and more meaningful, we need to avoid the introduction of a new filter or attribute that is a duplicate or redundant. This work is an attempt at such a practice in using the 2D and 3D vectors and their attributes.

ACKNOWLEDGMENTS

We would like to thank O. Boulanger, reviewers G. R. J. Cooper, M. C. Hidalgo-Gato, M. Nabighian, and S. V. Yalamanchili for their comments and suggestions that led to a significant improvement of this paper. We also acknowledge CGG and the Geological Survey of Canada for supporting this work and allowing its publication.

REFERENCES

Barnes, A. E., 2007, Redundant and useless seismic attributes: Geophysics, **72**, no. 3, P33–P38, doi: 10.1190/1.2716717.

Cooper, G. R. J., 2014, Reducing the dependence of the analytic signal amplitude of aeromagnetic data on the source vector direction: Geophysics, **79**, no. 4, J55–J60, doi: 10.1190/geo2013-0319.1.

Cooper, G. R. J., and D. R. Cowan, 2006, Enhancing potential field data using filters based on the local phase: Computers & Geosciences, **32**, 1585–1591, doi: 10.1016/j.cageo.2006.02.016.

Cooper, G. R. J., and R. C. Whitehead, 2016, Determining the distance to magnetic sources: Geophysics, **81**, no. 2, J25–J34, doi: 10.1190/geo2015-0142.1.

Cordell, L., and V. J. S. Grauch, 1985, Mapping basement magnetization zones from aeromagnetic data in the San Juan basin, New Mexico, *in* W. J. Hinze, ed., The utility of regional gravity and magnetic anomaly maps: SEG, 181–197.

Dalley, R. M., E. C. A. Gevers, G. M. Stampfli, D. J. Davies, C. N. Gastaldi, P. A. Ruijtenberg, and G. J. O. Vermeer, 1989, Dip and azimuth displays for 3D seismic interpretation: First Break, **7**, no. 3, 86–95.

Dickinson, J. L., J. R. Brewster, J. W. Robinson, and C. A. Murphy, 2009, Imaging techniques for full tensor gravity gradiometry data: 11th Biennial Technical Meeting, SAGA, Extended Abstracts, 84–88.

Evjen, H. M., 1936, The place of the vertical gradient in gravitational interpretations: Geophysics, **1**, 127–136, doi: 10.1190/1.1437067.

Felsberg, M., and G. Sommer, 2001, The monogenic signal: IEEE Transactions on Signal Processing, **49**, 3136–3144, doi: 10.1109/78.969520.

Felsberg, M., and G. Sommer, 2004, The monogenic scale-space: A unifying approach to phase-based image processing in scale-space: Journal of Mathematical Imaging and Vision, **21**, 5–26, doi: 10.1023/B:JMIV.0000026554.79537.35.

Grauch, V. J. S., M. R. Hudson, and S. A. Minor, 2001, Aeromagnetic expression of faults that offset basin fill, Albuquerque basin, New Mexico: Geophysics, **66**, 707–720, doi: 10.1190/1.1444961.

Hassan, H., and S. V. Yalamanchili, 2013, Monogenic signal decomposition: A new approach to enhance magnetic data: 83rd Annual International Meeting, SEG, Expanded Abstracts, 1206–1210.

Heiland, C. A., 1946, Geophysical exploration: Prentice-Hall Inc.

Hidalgo-Gato, M. C., and V. C. F. Barbosa, 2015, Edge detection of potential-field sources using scale-space monogenic signal: Fundamental principles: Geophysics, **80**, no. 5, J27–J36, doi: 10.1190/geo2015-0025.1.

Hsu, S.-K., J.-C. Sibuet, and C.-T. Shyu, 1996, High resolution detection of geologic boundaries from potential-field anomalies: An enhanced analytic signal technique: Geophysics, **61**, 373–386, doi: 10.1190/1.1443966.

Jacobsen, B. H., 1987, A case for upward continuation as a standard separation filter for potential-field data: Geophysics, **52**, 1138–1148, doi: 10.1190/1.1442378.

Li, X., 2006a, Understanding 3D analytic signal amplitude: Geophysics, **71**, no. 2, L13–L16, doi: 10.1190/1.2184367.

Li, X.., 2006b, On "Theta map: Edge detection in magnetic data" (C. Wijns, C. Perez, and P. Kowalczyk, 2005, Geophysics, **70**, no. 4, L39–L43): Geophysics, **71**, no. 3, X11, doi: 10.1190/1.2194525.

Li, X., 2008, Magnetic reduction-to-the-pole at low latitudes: Observations and considerations: The Leading Edge, **27**, 990–1002, doi: 10.1190/1.2967550.

Li, X., 2016, Terracing gravity and magnetic data using edge-preserving smoothing filters: Geophysics, **81**, no. 2, G37–G43, doi: 10.1190/GEO-2015-0409.1.

Luo, Y., M. Wang, F. Luo, and S. Tian, 2011, Direct analytic signal interpretation of potential field data using 2-D Hilbert transform: Chinese Journal of Geophysics, **54**, 551–559, doi: 10.1002/cjg2.v54.4.

MacLeod, I. N., S. Vierra, and A. C. Chaves, 1993, Analytic signal and reduction-to-the-pole in the interpretation of total magnetic field data at low magnetic latitudes: Proceedings of the 3rd International Congress of the Brazilian Society of Geophysicists, 830–835.

Miller, H. G., and V. Singh, 1994, Potential field tilt — A new concept for location of potential field sources: Journal of Applied Geophysics, **32**, 213–217, doi: 10.1016/0926-9851(94)90022-1.

Nabighian, M. N., 1972, The analytic signal of 2D magnetic bodies with polygonal cross-section: Its properties and use for automated anomaly interpretation: Geophysics, **37**, 507–517, doi: 10.1190/1.1440276.

Nabighian, M. N., 1974, Additional comments on the analytic signal of two dimensional magnetic bodies with polygonal cross-section: Geophysics, **39**, 85–92, doi: 10.1190/1.1440416.

Nabighian, M. N., 1984, Toward a three-dimensional automatic interpretation of potential field data via generalized Hilbert transforms: Fundamental relations: Geophysics, **49**, 780–786, doi: 10.1190/1.1441706.

Pilkington, M., and P. B. Keating, 2009, The utility of potential field enhancements for remote predictive mapping: Canadian Journal of Remote Sensing, **35**, S1–S11, doi: 10.5589/m09-021.

Riesz, M., 1928, Sur les fonctions conjuguées: Mathematische Zeitschrift, **27**, 218–244, doi: 10.1007/BF01171098.

Roest, W. R., J. Verhoef, and M. Pilkington, 1992, Magnetic interpretation using the 3D analytic signal: Geophysics, **57**, 116–125, doi: 10.1190/1.1443174.

Stein, E. M., and G. Weiss, 1971, Introduction to Fourier analysis on Euclidean spaces: Princeton University Press.

Taner, M. T., F. Koehler, and R. E. Sheriff, 1979, Complex seismic trace analysis: Geophysics, **44**, 1041–1063, doi: 10.1190/1.1440994.

Thurston, J. B., and R. S. Smith, 1997, Automated conversion of magnetic data to depth, dip and susceptibility contrast using the SPI(TM) method: Geophysics, **62**, 807–813, doi: 10.1190/1.1444190.

Ulrych, T., M. Sacchi, M. Graul, and M. T. Taner, 2007, Instantaneous attributes: The what and the how: Exploration Geophysics, **38**, 213–219, doi: 10.1071/EG07023.

Wijns, C., C. Perez, and P. Kowalczyk, 2005, Theta map: Edge detection in magnetic data: Geophysics, **70**, no. 4, L39–L43, doi: 10.1190/1.1988184.